Highly efficient second-harmonic generation in buried waveguides formed by annealed and reverse proton exchange in periodically poled lithium niobate

Krishnan R. Parameswaran, Roger K. Route, Jonathan R. Kurz, Rostislav V. Roussev, and Martin M. Fejer

Edward L. Ginzton Laboratory, Stanford University, Stanford, California 94305-4085

Masatoshi Fujimura

Department of Electronics, Osaka University, Osaka 565-0871, Japan

Received October 2, 2001

Efficient three-wave mixing devices have numerous applications, including wavelength conversion, dispersion compensation, and all-optical switching. Second-harmonic generation (SHG) is a useful diagnostic for near-degenerate operation of these devices. With buried waveguides formed in periodically poled lithium niobate by annealed and reverse proton exchange, we demonstrate what is believed to be the highest normalized conversion efficiency (150%/W cm^2) for SHG in the 1550-nm communications band reported to date. © 2002 Optical Society of America

OCIS codes: 190.2620, 190.4360.

Optical frequency mixers have recently been shown to have many applications in communications, including wavelength conversion in wavelength-division multiplexed systems and multiplexing of high-speed time-division multiplexed signals.[1] These devices use near-degenerate three-wave mixing in guided-wave quasi-phase-matched interactions. The waveguides in these experiments were made by annealed proton exchange in periodically poled lithium niobate (PPLN). Proton exchange is a surface diffusion process that produces a step-index profile in the substrate. Subsequent annealing results in a graded-index profile whose maximum is constrained to be at the surface, such that the resulting mode profiles are highly asymmetric in depth.

We present measurements of linear and nonlinear optical properties of buried waveguides formed by annealed proton exchange followed by reverse proton exchange in PPLN. The symmetry and preservation of material nonlinearity provided by the buried waveguide results in a more-than-threefold improvement in conversion efficiency over that of annealed-proton-exchanged (APE) guides. A spatial mode image is presented, along with a second-harmonic-generation (SHG) tuning curve, for which a peak normalized conversion efficiency of 150%/W cm^2 is observed.

SHG is a useful diagnostic for three-wave mixing interactions. The amount of second-harmonic power, $P_{2\omega}$, generated in a waveguide of length L in the undepleted-pump limit (neglecting propagation loss) is given by

$$P_{2\omega}(L) = \eta_{\mathrm{nor}} L^2 [P_{\omega}(0)]^2, \tag{1}$$

where

$$\eta_{\mathrm{nor}} \propto \frac{{d_{\mathrm{eff}}}^2 |\vartheta|^2}{n^3}, \tag{2}$$

$$\vartheta = \iint_{-\infty}^{\infty} d(x,y)[A_{\omega}(x,y)]^2 A_{2\omega}(x,y)\mathrm{d}x\mathrm{d}y, \tag{3}$$

where η_{nor} [1/W cm^2] is the normalized SHG conversion efficiency, d_{eff} [m/V] is the effective nonlinear coefficient of the substrate, n is the effective index of the transverse mode at the fundamental frequency, ϑ [1/m] is the overlap integral of the interacting waveguide modes, $d(x,y)$ is the value of the nonlinear coefficient in the waveguide normalized to that in the substrate (and thus ranging from 0 to 1), and $A(x,y)$ represent the spatial profiles of the transverse waveguide modes normalized to unit power at the two wavelengths. The efficiency of near-degenerate three-wave mixing (where two of three waves are at similar wavelengths) is identical to η_{nor} for SHG given in Eq. (1), with $[P_{\omega}(0)]^2$ replaced with the product of the powers at the two input frequencies. Hence, SHG is useful for characterizing these devices for other interactions.

Proton exchange involves immersion of the PPLN substrate in a molten acid, such that H^+ ions (protons) in the melt are exchanged with Li^+ ions in the crystal. This process results in a thin proton-rich surface layer that has a higher extraordinary index than the substrate ($\Delta n_e = 0.09$ at 1550 nm), forming a waveguide for one polarization. Studies of the linear and nonlinear properties of these proton-exchanged waveguides show that, while they provide strong optical confinement (which increases the efficiency of nonlinear mixing processes), they are also relatively lossy [0.5–1 dB/cm (Ref. 2)] and exhibit near-complete

0146-9592/02/030179-03$15.00/0

erasure of the second-order nonlinear susceptibility [$d(x, y) \approx 0$ (Ref. 3)], forming a dead layer. The overlap integral, ϑ, and thus the SHG efficiency, η_{nor}, are reduced by this phenomenon. Annealing leads to the diffusion of protons deeper into the substrate, such that the peak Δn_e is reduced and the material phase changes into one exhibiting lower loss (the so-called α phase[2]). This diffusion of protons is accompanied by a partial recovery of the nonlinear coefficient within the initial exchanged layer.[3] Hence, we can optimize mixers based on APE waveguides by choosing the surface index to be as high as possible (to provide strong confinement) while still being in the low-loss α phase. This approach leads to conversion efficiencies of the order of $\eta_{\mathrm{nor}} \approx 40\%/\mathrm{W\ cm^2}$.[1]

One difficulty with APE waveguides is that the index profile is constrained to have a maximum at the surface and to decrease monotonically into the substrate; hence, it is highly asymmetric in the depth dimension. Since the SHG and fundamental wavelengths differ by a factor of two, this asymmetry results in modes whose maxima do not coincide in depth. Making the waveguide symmetric can eliminate this problem. Removal of protons from the waveguide surface lowers the refractive index near the surface, shifting the maxima of the modes deeper into the substrate (and away from the dead layer), while simultaneously forcing the peaks of the modes to coincide in depth. This reverse exchange can be accomplished by immersion of the sample in a lithium-rich melt such that protons diffuse out of the PPLN and are replaced by lithium ions. An additional advantage of this process is that the spatial modes of channel waveguides can be engineered to be symmetric in both width and depth, leading to better overlap with optical fiber modes. Several groups have explored this process and observed its attractive properties, including recovery of the nonlinear coefficient[4,5] and symmetry of spatial modes.[6,7]

Device fabrication began with electric field poling[8] of a 7.62-cm-diameter lithium niobate wafer with multiple quasi-phase-matching periods. Waveguides of various widths were formed in a direction orthogonal to the quasi-phase-matching gratings, and mode filters and tapers were used to facilitate launching into the fundamental transverse modes of the waveguides.[9] A 3.3-cm-long sample was diced out of the wafer, then proton exchanged for 31 h at 160 °C in pure benzoic acid, resulting in a film of approximately 1-μm thickness. The sample was then annealed in air for 8 h at 328 °C. Subsequent reverse exchange involved immersion of the sample in a eutectic melt of $LiNO_3$:KNO_3:$NaNO_3$ in a mole percent ratio of 37.5:44.5:18.0 (Ref. 7) for 10 h at 328 °C. Exchange in pure $LiNO_3$ has been found to damage the $LiNbO_3$ surface, whereas the mixed nitrate melt does not do so.[6] Containing the melt in a quartz beaker inside a cylindrical tube furnace maximized the temperature uniformity. Using a proven empirical model for the diffusion of protons into and out of lithium niobate,[10] we chose the above-described combination of proton-exchange, annealing, and reverse-exchange parameters so that the peak concentration after reverse exchange was roughly one fourth that of the as-exchanged material (which ensured that the entire waveguide was in the low-loss phase[2]). We then polished the sample end faces at 90° to facilitate end-fire coupling.

Figure 1 shows an image of the spatial mode at 1536.5 nm of a 7-μm-wide buried waveguide. A slice in the vertical (depth) direction is also shown, where the ratio of the $1/e^2$ half-widths is nearly 1:1. This ratio is much better than that of typical APE waveguides (2.8:1), in which the asymmetric diffusion results in a long tail in depth. A SHG tuning curve for a quasi-phase-matching period of 15.5 μm is shown in Fig. 2. The peak normalized conversion efficiency is $150\%/\mathrm{W\ cm^2}$, more than three times that of typical devices ($38\%/\mathrm{W\ cm^2}$, as described in Ref. 11), and to our knowledge the highest ever observed for SHG in this wavelength band. The tuning curve has a nearly ideal sinc^2 shape, indicating that phase matching is maintained throughout the device length. Figure 3 shows a plot of the phase-matching wavelength as a function of waveguide width, confirming that a dimensionally noncritical point occurs at a width near 8 μm.

A 6-cm-long waveguide with this value of η_{nor} would have an efficiency of 5400%/W. It is instructive to examine the wavelength-conversion efficiency

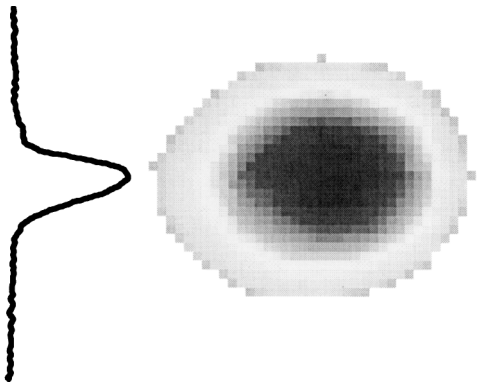

Fig. 1. Spatial mode and vertical cross section, showing symmetry in depth.

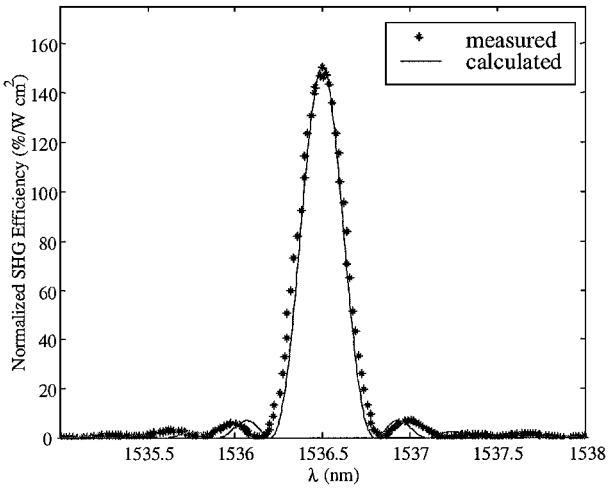

Fig. 2. Measured and calculated cw SHG tuning curve for a 3.3-cm-long waveguide.

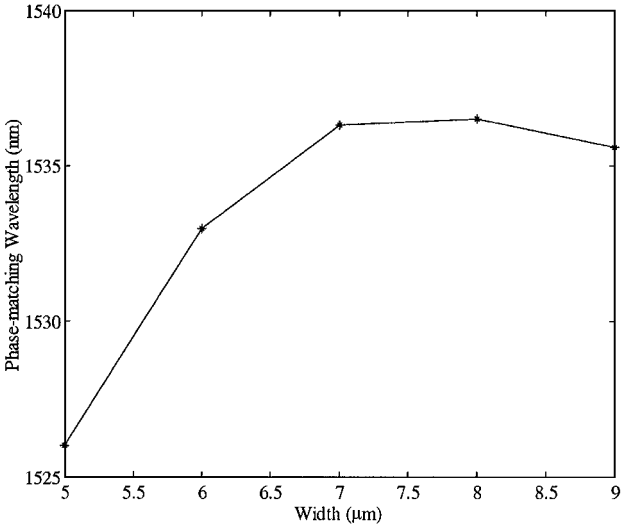

Fig. 3. Measured phase-matching wavelength versus waveguide width, showing noncritical phase matching at a width of 8 μm.

and parametric gain that can be obtained through near-degenerate difference-frequency generation in such a device. With a pump input in the 775-nm band (a configuration presented in Ref. 12), wavelength conversion within the 1550-nm band with 0-dB conversion loss can be obtained with only 30 mW of pump power. This calculation accounts for pump depletion and assumes typical propagation losses of 0.3 dB/cm at 1550 nm and 0.6 dB/cm at 775 nm. Signal parametric gain of 10 dB would be obtained with 115-mW pump power. In a cascaded configuration, SHG of an input local oscillator at 1550 nm generates the pump at 775 nm. This pump simultaneously mixes with an input signal through difference-frequency generation to create the wavelength-converted output.[9] In this configuration, 0-dB conversion loss and 10-dB parametric gain require 75- and 192-mW input local-oscillator power at 1550 nm, respectively.

This work was supported by the Defense Advanced Research Projects Agency through the Optoelectronics Materials Center, by the National Science Foundation through contract ECS-9903156, and by the U.S. Air Force Office of Scientific Research through contract 49620-99-1-0270. K. Parameswaran's e-mail address is krishp@stanford.edu.

References

1. M. H. Chou, K. R. Parameswaran, I. Brener, and M. M. Fejer, IEICE Trans. Electron. **E83C,** 869 (2000).
2. Yu. N. Korkishko, V. A. Fedorov, M. P. de Micheli, P. Baldi, K. El Hadi, and A. Leycuras, Appl. Opt. **35,** 7056 (1996).
3. M. L. Bortz, L. A. Eyres, and M. M. Fejer, Appl. Phys. Lett. **62,** 2012 (1993).
4. J. Rams, J. Olivares, and J. M. Cabrera, Electron. Lett. **33,** 322 (1997).
5. Yu. N. Korkishkov, V. A. Fedorov, and F. Laurell, IEEE J. Sel. Top. Quantum Electron. **6,** 132 (2000).
6. J. L. Jackel and J. J. Johnson, Electron. Lett. **27,** 1360 (1991).
7. Yu. N. Korkishkov, V. A. Fedorov, T. M. Morozova, F. Caccavale, F. Gonella, and F. Segato, J. Opt. Soc. Am. A **15,** 1838 (1998).
8. L. E. Myers, R. C. Eckardt, M. M. Fejer, R. L. Byer, W. R. Bosenberg, and J. W. Pierce, J. Opt. Soc. Am. B **12,** 2102 (1995).
9. M. H. Chou, I. Brener, M. M. Fejer, E. E. Chaban, and S. B. Christman, IEEE Photon. Technol. Lett. **11,** 653 (1999).
10. M. L. Bortz and M. M. Fejer, Opt. Lett. **16,** 1844 (1991).
11. K. R. Parameswaran, J. R. Kurz, R. V. Roussev, and M. M. Fejer, Opt. Lett. **27,** 43 (2002).
12. M. H. Chou, J. Hauden, M. A. Arbore, and M. M. Fejer, Opt. Lett. **23,** 1004 (1998).